
Simulation of a Boomerang's Trajectory

Group Members:

*Fu Minqi
Jia Xiaohe
Zhang Yuxuan*

Instructor:

Dr. Guan Chun

School:

Beijing National Day School

Location:

Beijing, China



DONGRUN-YAU SCIENCE AWARD
DECEMBER 2016

Statement of Originality

This team declares that the submitted paper is the result of the research done in the supervision of the advisor. To this team's knowledge, apart from the contents that are in-text cited or listed in acknowledgement, this paper does not include any research from others' work or from anything this team has written or has published. If our statement is anyway untrue, we bear all legal responsibilities.

Signatures:
Minqi Fu Xiaohe Jia
Yuxuan Zhang
Date: Dec. 9, 2016

Abstract

This research is dedicated to model the trajectory of two-armed boomerangs with its known parameters. In the theoretical model, we disassembled the boomerang's complex motion into three aspects: vertical displacement, horizontal velocity, and vector radius, and provided theoretical basis to develop functions for each of the parts. In our model, we took into account several forces and variables that are overlooked by previous quantified studies, aiming to predict a boomerang's flight path by its physical properties and initial velocities.

Besides the theoretical model, this research also involves two experiments. In the first experiment, a wind tunnel is used to simulate the flight conditions. A boomerang fixed on a experiment apparatus was placed inside the wind tunnel. The boomerang's angular velocity, linear velocity, as well as its torque, was measured at several different levels. Also, by changing the boomerang's directions to the wind, we can measure the torques resulted by various factors. Thus, combined with the theoretical model, constant values that affects its flight can be calculated for such a boomerang.

In the second experiment, we recorded the video of a boomerang's flight. In this case, the position of the thrower and the cameras were intentionally designed. Hence, with the aid of referencing objects on the boomerang's path, we were able to measure the change of angles of inclination and radius, which was used to verify our theoretical model and provides the basis for the simulation program. The program could plot a precise 2D trajectory if the initial horizontal velocity and angular velocity is known.

Contents

1	Introduction	4
1.1	Background Information	4
1.2	List Variables and Constants	6
2	Theoretical Model	7
2.1	Overview	7
2.2	Radius of Curvature	9
2.3	Direction of Radius	10
2.4	Motion in the Vertical Direction	11
2.5	Simplified Theory	12
3	Experiments	13
3.1	Wind Tunnel Experiment	13
3.1.1	Experiment Overview	13
3.1.2	Experiment Setup	13
3.2	Data Analysis	16
3.2.1	Trail 1, 2 and lift coefficient	16
3.2.2	Trail 4, 5 and drag coefficient	18
3.2.3	Error analysis	19
3.2.4	Solve differential equation using Mathematica	20
3.2.5	Approaches to account for the Different result of $ R $	22
3.3	Experiment account for $\alpha(t)$	23
3.3.1	Experiment objective	23
3.3.2	Experiment setup	23
3.4	Data Calculation	23
3.5	Data analysis	25
3.5.1	Verification of the theoretical model of $\omega(t)$ and $v_h(t)$	25
3.5.2	Numerical solution of $ R $ and α	26
3.5.3	Simulation	28
3.5.4	Significance	29
4	Conclusion	30
5	Appendix	31
5.1	Mathematica Codes	31

1 Introduction

1.1 Background Information

A “boomerang” generally refers to a simple aerodynamically designed object that makes a quasi-circular flight and roughly returns to its starting point when thrown correctly. Examples of different types of boomerangs are illustrated in Figure 1. This paper focuses on traditional V-shaped boomerangs which resemble the modern aboriginal boomerangs in Figure 1.



Figure 1: Types of boomerangs (Vassberg, 2012)

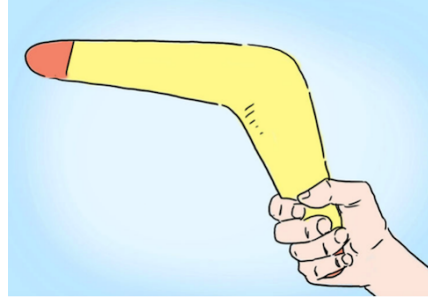


Figure 2: Correct way to hold a boomerang (Vassberg, 2012)

Historically, boomerangs are developed from kylies which were used as hunting weapons in several culture groups across the world. In spite of the popular association of boomerangs to Australian aborigines, evidence suggests that boomerangs may have emerged from early civilizations like Egypt and Indian (Humble, 2006). For the convenience of discussion, different parts of a boomerang are going to be referred to as the names indicated in Figure 3.

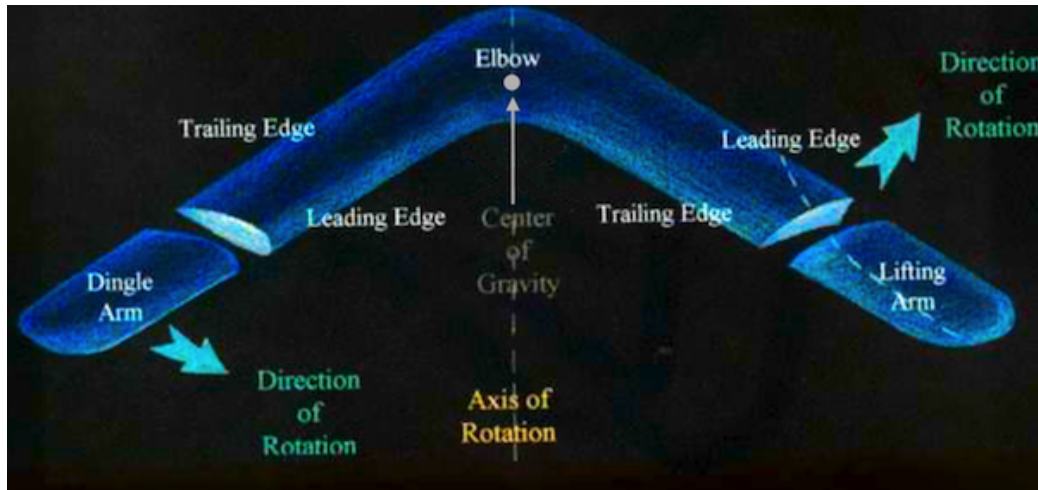


Figure 3: Names of parts on a two-armed boomerang (Hawes, 1987)

The boomerang in Figure 3 is right-handed, which means a person should throw it with the right hand and its trajectory is counterclockwise, vise versa with left-handed boomerangs. A left-handed boomerang differs from the one in Figure 3 only by switching the leading and trailing edges of each arm. To correctly throw a boomerang, one should hold it as demonstrated in Figure 2, with the flat side of the boomerang facing into the page. Using the wrist to give it a spin, the initial angular velocity in this case should be the sum of two vectors,

one out of the page and one to the top of the page. The angular velocity should always be perpendicular to the plane that the boomerang is on if it is regarded as the 2 dimensional surface of its flat side. Using a person's arm to propel it forward, the initial linear velocity in this case should also be the sum of two vectors, one to the left of the page and one to the top of the page. Previous works on the aerodynamics of boomerangs done by Hugh Hunt quantitatively offer a rough estimate of the trajectory in a 2 dimensional plane (Hunt, 2001). Most of the currently published explanations of the motion of boomerangs are qualitative. Some examples are *Why Do Boomerangs Come Back?* by Yutaka Nishiyama, *Aerodynamics Of Boomerang* by Saulius Pakalnis, and *Flight Dynamics Of Boomerang* by Yong Suk Moon.

1.2 List Variables and Constants

The followings are all nomenclatures included in this paper:

- A : area of one arm of boomerang
- m : mass of boomerang
- $\vec{\omega}(t)$: angular velocity of boomerang
- $\alpha(t)$: angle between boomerang's angular velocity and the horizontal plane
- $\vec{v}_h(t)$: the component of linear velocity on x-y plane
- $\vec{v}_v(t)$: the component of linear velocity in z-direction
- $\vec{R}(t)$: radius of boomerang's circular motion
- positive x-axis: coincides with $\vec{R}(0)$
- positive y-axis: coincides with $\vec{v}_h(0)$
- positive z-axis: cross product of x-axis and y-axis
- $\vec{F}_L(t)$: total lift force on boomerang
- $\vec{F}_D(t)$: horizontal drag force on boomerang
- $\vec{F}'_D(t)$: vertical drag force on boomerang
- ϕ : angle between two arms of boomerang
- r : arm length of boomerang
- $\theta(t)$: angle between dingle arm and horizontal axis in boomerang's plane
- $O(t)$: center boomerang's circular motion
- l : width of arms of boomerang
- $\beta(t)$: angle between \vec{R} and positive x-axis
- $\beta'(t)$: angle between x-y component of $\vec{\omega}(t)$ and positive x-axis
- ρ : air density
- C_{L1} : lift coefficient of lifting arm of boomerang
- $C_{L2}(t)$: lift coefficient of dingle arm of boomerang
- $\vec{F}_{L1}(t)$: lift force on lifting arm of boomerang
- $\vec{F}_{L2}(t)$: lift force on dingle arm of boomerang
- $\vec{\tau}_{L1}(t)$: torque on lifting arm of boomerang
- $\vec{\tau}_{L2}(t)$: torque on dingle arm of boomerang
- $\vec{F}_v(t)$: total force on boomerang in positive z direction
- C_D : drag coefficient when rotating boomerang is considered as a disk
- $\vec{\tau}_u(t)$: torque on perpendicular-to-horizontal axis on boomerang's plane
- $\vec{\tau}_s(t)$: torque horizontal axis on boomerang's plane
- $\vec{J}(t)$: angular momentum of boomerang
- A' : area of disk that boomerang makes when it rotates
- $\vec{\tau}_D(t)$: drag torque on boomerang
- $z(t)$: vertical displacement

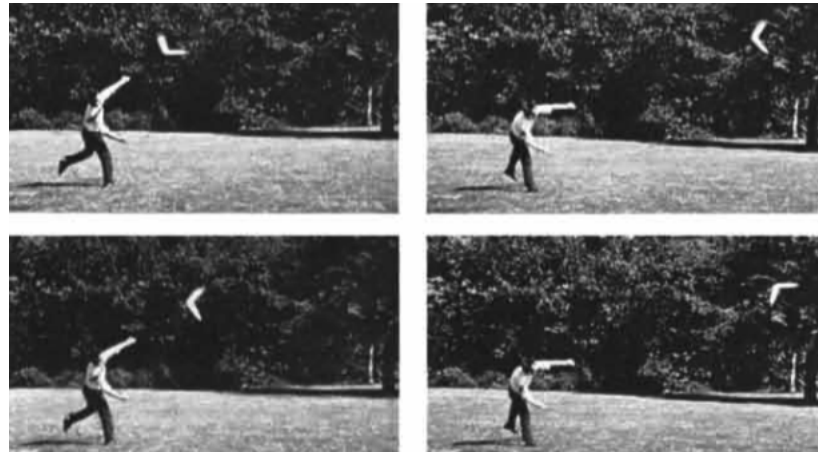


Figure 4: Snapshots of flying boomerangs (Hess, 1968)

2 Theoretical Model

2.1 Overview

To model the trajectory of a boomerang in 3 dimensions, computations are separated into 2 parts. The first one is the motion in the horizontal plane. The second one is the motion in the vertical direction.

In the following discussions, the boomerang's plane refers to the plane that the boomerang is on if it is regarded as the 2 dimensional surface of its flat side. For the derivation, it is assumed that the two arms of a given boomerang are identical, the center of mass is on the elbow and both the mass density and the shape of cross-sectional area is constant from the center of mass to the edge of each arm.

Through observations of snapshots of boomerangs in flight as shown in Figure 4, it is decided that it is adequate to assume that the boomerang's plane at any instant coincides with the vertical plane, that contains the boomerang's linear velocity, rotated at an angle α with the line that the horizontal component of the linear velocity is on, as the axis of rotation. In other words, there is no angle of elevation as the boomerang travels. As illustrated in Figure 5, α is the angle of inclination of the boomerang describing the angle between the boomerang's angular velocity and the horizontal plane. Figure 6 is a free-body diagram corresponding to the instant and viewing angle as that in Figure 6, the forces will be explained later.

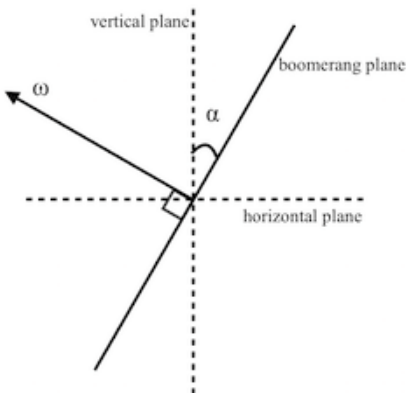


Figure 5: Angle of inclination

the horizontal plane. Figure 6 is a free-body diagram corresponding to the instant and viewing angle as that in Figure 6, the forces will be explained later.

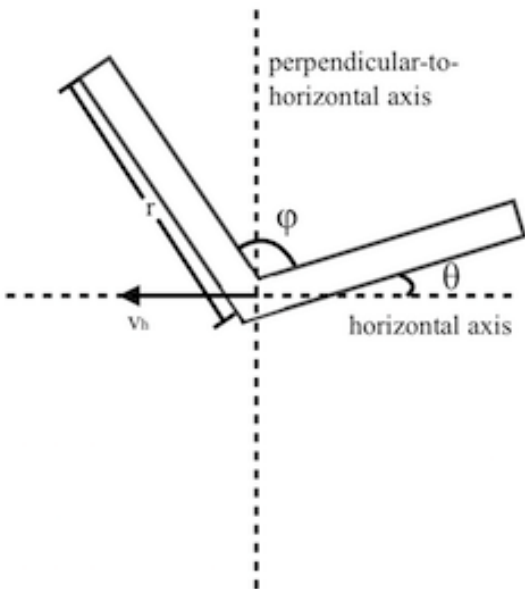


Figure 7: Boomerang's plane

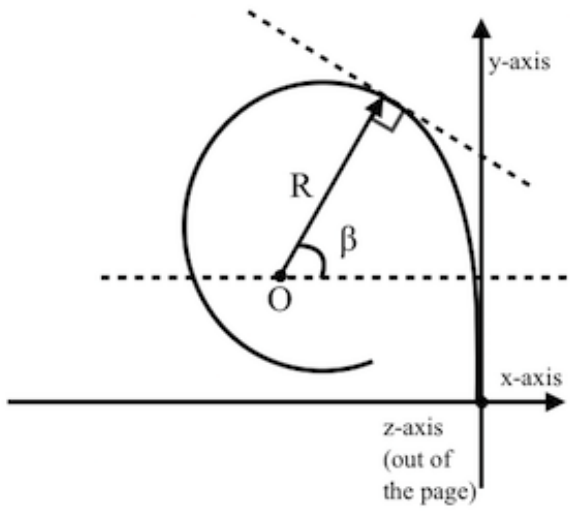


Figure 8: Boomerang's motion in horizontal plane

Figure 7 depicts the boomerang at an instant of time on its plane. v_h is the horizontal component of the linear velocity which is assumed to coincide with the horizontal axis on the boomerang's plane. θ is the angle between the dingle arm and the horizontal axis. Since the derivation is only connected with sines and cosines of θ , all $\theta \pm 2k$ (k is an integer) are equivalent. ϕ is the angle between two arms. r is the length from the center of mass to the edge of each arm.

In this theoretical model, the motion of the boomerang in the horizontal plane is approximated as the combination of an infinite amount of circular paths one in each infinitesimal amount of time. This is a plausible solution because the net force and the linear velocity of a boomerang is always approximately perpendicular to each other on the horizontal plane, for the horizontal drag force is relatively small. As illustrated in Figure 8, the two dimensional vector $\vec{R}(t)$ and its starting point $O(t)$ are both functions of time. \vec{R} at an instant in time is a vector defined by its length and the angle $\beta(t)$ it makes with positive x-axis with $\beta(0)$ being 0. Positive x-axis is horizontal and coincides with $\vec{R}(0)$, positive y-axis coincides with $\vec{v}_h(0)$, and z-axis is the cross products of x-axis and y-axis. Knowing $\vec{R}(t)$, $\vec{v}_h(t)$ and the vertical displacement $z(t)$, the trajectory of a boomerang could be modeled by imputing constants and initial conditions.

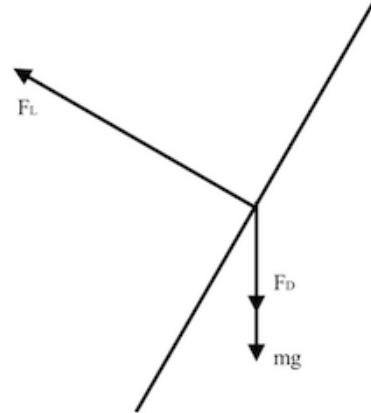


Figure 6: Free-body diagram

2.2 Radius of Curvature

According to the lift equation, the aerodynamic lift forces perpendicular to the plane of rotation of the airfoil are shown as follows.

$$\begin{aligned} F_{L1} &= \frac{1}{2}\rho C_{L1} l \int_0^r (v_h \sin(\phi + \theta)) + r\omega)^2 dr \\ &= \frac{1}{2}\rho C_{L1} l(v_h^2 r \sin^2(\phi + \theta) + v_h r^2 \omega \sin(\phi + \theta) + \frac{1}{3}r^3 \omega^2) \\ F_{L2} &= \frac{1}{2}\rho C_{L2} l \int_0^r (v_h \sin \theta + r\omega)^2 dr \\ &= \frac{1}{2}\rho C_{L2} l(v_h^2 r \sin^2 \theta + v_h r^2 \omega \sin \theta + \frac{1}{3}r^3 \omega^2) \end{aligned} \quad (1)$$

The total lift F_L is shown below.

$$F_L = F_{L1} + F_{L2} \quad (2)$$

Since on the horizontal surface, the centripetal force $F_L \cos \alpha$ is always perpendicular to the linear velocity, Newton's Second Law Of Motion could be used v_h .

$$F_L \cos \alpha = m \frac{v_h^2}{|\vec{R}|} \quad (3)$$

Since lift coefficient C_L depends on various factors such as air viscosity, air density, shape of airfoil, it could vary over time. There is disturbance of air in front of the direction of travel of the dingle arm, since the lifting arm travels pass that area. The disturbance of air in front of the lifting arm can be ignored because $(2\pi - \phi)$ is much bigger than ϕ . Considering the disturbance that affects air viscosity and the fact that an arm has higher velocity when it is above the horizontal plane, C_{L2} could be modeled by a graph as shown in Figure 9. A good approximation of such a graph is $C_{L2}(t) = C_1 - C_2 \cos \theta - \cos^2 \theta$ where C_1 and C_2 are positive constants that will be determined experimentally. C_{L1} is just modeled a constant that will also be determined experimentally, since its fluctuation is much smaller than C_{L2} 's and could be ignored.

$F_L(t)$ could be written entirely as a function of the after finding out $\vec{v}_h(t)$, $\omega(t)$ and $\theta(t)$.

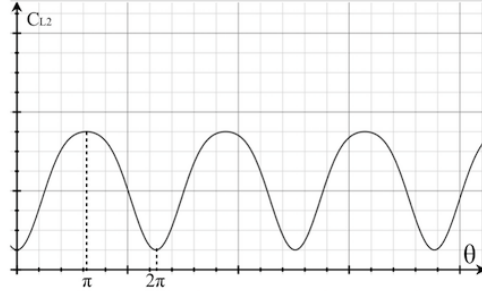


Figure 9: Approximation of C_{L2} vs θ

To find $\vec{v}_h(t)$, use the drag force equation and Newton's Second Law of Motion as shown below.

$$\begin{aligned} F'_D &= \rho C_D l \int_0^r (v_h \sin(\phi + \theta)) + r\omega)^2 dr \\ -m \frac{dv_h}{dt} &= \rho C_D l (v_h^2 r \sin^2(\phi + \theta) + v_h r^2 \omega \sin(\phi + \theta) + \frac{1}{3} r^3 \omega^2) \\ -\frac{dv_h}{dt} &= \frac{\rho C_D A}{m} (v_h^2 \sin^2(\phi + \theta) + v_h r \omega \sin(\phi + \theta) + \frac{1}{3} r^2 \omega^2) \end{aligned} \quad (4)$$

Using the drag force equation for torque and Newton's Second Law for circular motion, the following shows steps to calculate $\omega(t)$. Then $\theta(t) = \int_0^t \omega(t) + \theta(0)$.

$$\begin{aligned} \tau_D &= \rho C_D l \int_0^r (v_h \sin \theta + r\omega)^2 r dr \\ -I \frac{d\omega}{dt} &= \rho C_D l (\frac{1}{2} v_h^2 r^2 \sin^2 \theta + \frac{2}{3} v_h r^3 \omega \sin \theta + \frac{1}{4} r^4 \omega^2) \\ -\frac{d\omega}{dt} &= \frac{\rho C_D A}{I} (\frac{1}{2} v_h^2 r \sin^2 \theta + \frac{2}{3} v_h r^2 \omega \sin \theta + \frac{1}{4} r^3 \omega^2) \end{aligned} \quad (5)$$

2.3 Direction of Radius

This section includes the formula derivation of the torque that makes the boomerang change its $\beta(t)$, the direction of radius, and the first of two explanations of the change of α , the angle of inclination, with time. The other explanation is a little bit more complex and is explicitly stated in subsection 3.4. Because both of the derivations are convincing, it is hard to abandon either.

After finding F_L , $\vec{R}(t)$ could be determined by calculating $\alpha(t)$ and $\beta(t)$. First, use the same equation as the one used to calculate F_L , $F_L = \rho v^2 C_L A$. The torque on the lifting arm and dingle arm, τ_{L1} and τ_{L2} are given by the following equations.

$$\begin{aligned} \tau_{L1} &= \frac{1}{2} \rho C_{L1} l \int_0^r ((v_h \sin(\phi + \theta)) + r\omega)^2 r dr \\ &= \frac{1}{2} \rho C_{L1} l (\frac{1}{2} v_h^2 r^2 \sin^2(\phi + \theta) + \frac{2}{3} v_h r^3 \omega \sin(\phi + \theta) + \frac{1}{4} r^4 \omega^2) \\ \tau_{L2} &= \frac{1}{2} \rho C_{L2} l \int_0^r (v_h \sin \theta + r\omega)^2 r dr \\ &= \frac{1}{2} \rho C_{L2} l (\frac{1}{2} v_h^2 r^2 \sin^2 \theta + \frac{2}{3} v_h r^3 \omega \sin \theta + \frac{1}{4} r^4 \omega^2) \end{aligned} \quad (6)$$

The torque on the perpendicular-to-horizontal axis shown in Figure 7, is shown as below.

$$\tau_u = -\tau_{L1} \cos(\phi + \theta) - \tau_{L2} \cos \theta \quad (7)$$

The torque on the horizontal axis show in Figure 7, is shown as below.

$$\tau_s = \tau_{L1} \sin(\phi + \theta) + \tau_{L2} \sin \theta \quad (8)$$

According to the circular-motion variation of Newton's Second Law Of Motion, $\tau = \frac{dJ}{dt}$. As shown in Figure 10, an arc approximation gives $dJ\alpha = \tau_u dt$, since $J = I\omega$,

$$\alpha(t) = \int_0^t \frac{\tau_u dt}{I\omega(t)} + \alpha(0). \quad (9)$$

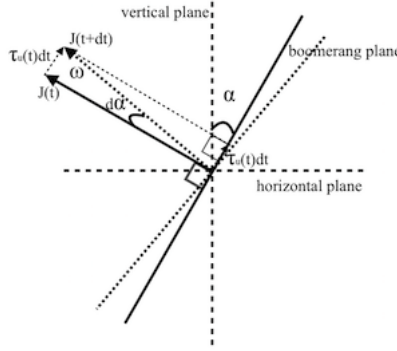


Figure 10: Change of angular momentum

$\beta(t)$ could be obtained from similar methods as $\alpha(t)$.

$$\beta(t) = \int_0^t \frac{\tau_s dt}{I\omega(t)\cos(\alpha(t))} \quad (10)$$

With the formulas of $\alpha(t)$ and $\beta(t)$, R can be derived as follows. At any instant, the path of the boomerang is approximately an arc where $v_h d\theta = R dt$, combined with the equation of $\beta(t)$ above $\vec{R}(t)$ is now a function of time with all other parameters as constants.

$$R = \frac{3I\cos\alpha}{\rho C_L A r^2} \quad (11)$$

2.4 Motion in the Vertical Direction

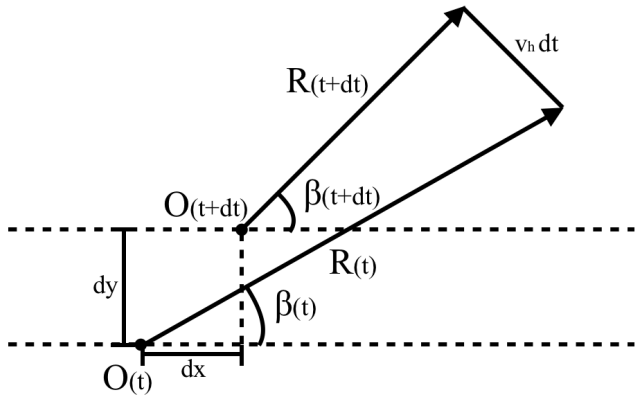


Figure 11: Solving for $x(t)$ and $y(t)$

Now that $\vec{R}(t)$ and $v_h(t)$ is determined, the only thing left is $z(t)$. Figure 11 could be solved by a computer program at every instant in time to find $x(t)$ and $y(t)$.

Finally, $z(t)$ is derived from the vertical component of F_L and the boomerang's weight. The vertical drag force due to the vertical velocity is ignored since the vertical velocity is small. As shown in Figure 6, the total upward force, in the positive z-axis is given by the following.

$$F_v(t) = F_L \sin \alpha - mg \quad (12)$$

Using Newton's Second law of Motion, $F_v = m \frac{dv_v}{dt}$, so $v_v(t)$ could be solved accordingly. Then

$$z(t) = \int_0^t v_v(t) dt \quad (13)$$

$$z(t) = gt^2 + \int_0^t \int_0^t \frac{\rho C_L A}{2m} v_h^2 \sin \alpha dt^2 + \int_0^t \int_0^t \frac{\rho C_L A}{3m} r^2 \omega^2 \sin \alpha dt^2 \quad (14)$$

At this point, every equation necessary to model the trajectory of a boomerang has been shown. We are going to simplify these in order to do experiments and make a computer program.

2.5 Simplified Theory

In order to test our theory by accessible equipments, we made the following reasonable approximations to simplify it.

First, we ignore the minor fluctuation of the boomerang on z direction for the first experiment, so the trajectory is modeled in 2-dimension. Second, we assume the angle of inclination, α is constant also for the first experiment. Third, we ignore the minimal effect of disturbance and assume C_L and C_D to be constant and the same on both arms for both experiments.

Simplifying our equations from previous sections by averaging sins to 0, \sin^2 s to 1 and \sin^3 s to 0, we get the following equations to calculate $\vec{R}(t)$.

$$\begin{aligned} F_L &= \rho C_L l \int_0^r (v_h \sin \theta + r\omega)^2 dr \\ &= \rho C_L A (v_h^2 \sin^2 \theta + v_h r \omega \sin \theta + \frac{1}{3} r^2 \omega^2) \\ &\approx \rho C_L A (\frac{1}{2} v_h^2 + \frac{1}{3} r^2 \omega^2) \\ F_L \cos \alpha &= m \frac{v_h^2}{|\vec{R}|} = \rho C_L A (\frac{1}{2} v_h^2 + \frac{1}{3} r^2 \omega^2) \cos \alpha \end{aligned} \quad (15)$$

$$\begin{aligned} \tau_L &= \sin(\theta) \rho C_L l \int_0^r (v_h \sin \theta + r\omega)^2 r dr \\ &= \rho C_L A (\frac{1}{2} v_h^2 r \sin^3 \theta + \frac{2}{3} v_h r^2 \omega \sin^2 \theta + \frac{1}{4} r^3 \omega^2 \sin \theta) \\ &\approx \rho C_L A (\frac{1}{3} v_h r^2 \omega) \end{aligned} \quad (16)$$

$$\begin{aligned} \tau_D &= \rho C_D l \int_0^r (v_h \sin \theta + r\omega)^2 r dr \\ -I \frac{d\omega}{dt} &= \rho C_D l (\frac{1}{2} v_h^2 r^2 \sin^2 \theta + \frac{2}{3} v_h r^3 \omega \sin \theta + \frac{1}{4} r^4 \omega^2) \\ -\frac{d\omega}{dt} &\approx \frac{\rho C_D A}{I} (\frac{1}{4} v_h^2 r + \frac{1}{4} r^3 \omega^2) \end{aligned} \quad (17)$$

$$\begin{aligned} F_D &= \rho C_D l \int_0^r (v_h + r\omega \sin \theta)^2 dr \\ -m \frac{dv_h}{dt} &= \rho C_D l (v_h^2 r + v_h r^2 \omega \sin \theta + \frac{1}{3} r^3 \omega^2 \sin^2 \theta) \\ -\frac{dv_h}{dt} &\approx \frac{\rho C_D A}{m} (v_h^2 + \frac{1}{6} r^2 \omega^2) \end{aligned} \quad (18)$$

$$\begin{aligned} \beta(t) &= \int_0^t \frac{\tau_L dt}{I \omega(t) \cos \alpha} \\ \beta(t) &= \int_0^t \frac{\rho C_L A v_h r^2 dt}{3 I \cos \alpha} \end{aligned} \quad (19)$$

Using the information for $\vec{R}(t)$, $\vec{v}_h(t)$ and $z(t)$ the simplified trajectory of a boomerang could be modeled by Mathematica after inserting constants as shown in the following sections.

3 Experiments

3.1 Wind Tunnel Experiment

3.1.1 Experiment Overview

In the experiment part, we simulated a chosen boomerang at an instant in time for real-life flight situations, and we also throw the boomerang with different initial parameters. Both of the experiment are designed for two purposes: to prove the theoretical basis in the previous section and to measure C_D and C_L for a boomerang.

3.1.2 Experiment Setup

In order to control parameters such as velocity of the boomerang, we conducted the experiment in a small wind tunnel. The structure of the wind tunnel is shown in Fig 13. A series of 0.6m-wide plastic pipe were arranged in line on wooden stands, which serves as the tunnel for the wind to go through. A fan was set at one end of the tunnel; the fan was connected to a voltage transformer from 0V to 220V so that we can adjust its the wind speed by changing the voltage output.

Since the wind created by a fan is usually inconstant, in order to overcome this defect, first, the wind tunnel is made 5 meters long and the boomerang was placed at the other end of the tunnel from the fan, so the distance can serve as a buffer for the nonuniform air to adjust itself; also, to help stabilize the flow, we inserted a plastic honeycomb cover between the boomerang and the fan. According to the article: *Construction and Stabilization of Small-scale Wind Tunnel*, the honeycomb-shaped structure, as shown in Fig 12, can help reduce vortex effect in the tunnel.



Figure 12: The wind tunnel setup

As shown in Figure 13, the boomerang itself is fixed on a metal rotating axle. Since we assume in our calculation that the boomerang always rotate around its center of mass, and the actual location of its center is between its two arms, we clipped the boomerang using a clamp so that the center of mass of the boomerang is approximately on the rotating axle.

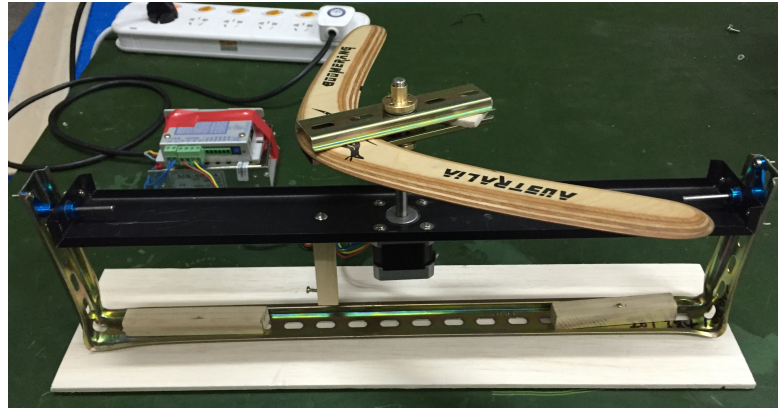


Figure 13: The torque measuring device

The metal axle (the horizontal axle) is fixed on the sides of a U-shaped metal frame which is fastened on a wooden base so the whole structure can stand steadily. The top board is a black metal plate which is able to rotate freely around the horizontal axle because two bearings connect them, and the top board's lower tip is connected to a small step motor inside the frame. This step motor powers the rotation of the rotating axle and the boomerang. It is also connected with a controller which is able to change the frequency of the output signal in order to simulate angular velocity ω into different magnitudes. the controller is connected to a voltage transformer so that it is able to work in a proper voltage.

A wooden block is placed under this side of the top board, and a string is fixed on the wooden block. The string goes through a pulley and is connected to some weight on an electronic scale as shown in Figure 15. The center of mass of the top board, the step motor, the boomerang and the wooden block is adjusted exactly on the horizontal axle so as to reduce the error caused by extra torque.

When the boomerang rotates, its tendency to rotate around the top board would be stopped by the string's tension, which lifts the weights and results in a change in the electronic scale's reading.

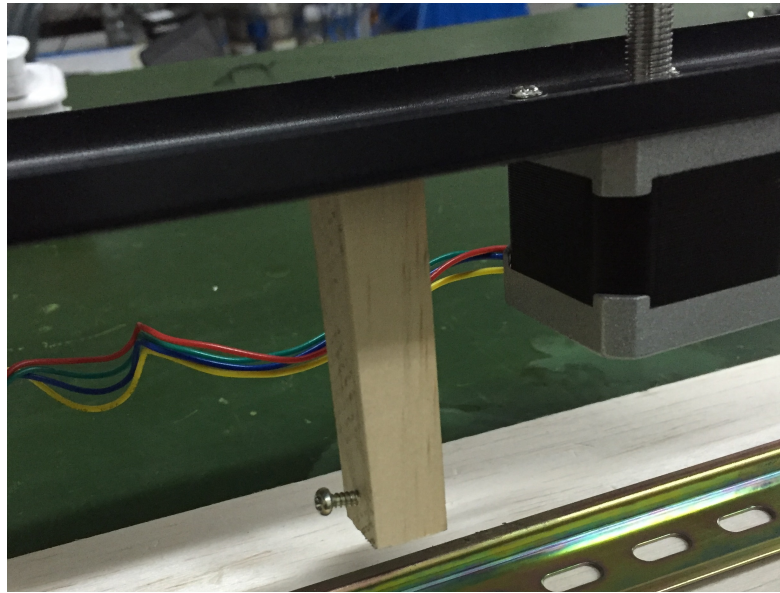


Figure 14: Measuring Part

Using the equipments introduced above, we have got five sets of data of different condition. Before the actual trials, with only the fan and the wind tunnel, starting at 75 V, open the fan and use an anemometer to measure the wind velocity and the boomerang site until the speed stabilizes. Then change the voltage and repeat such procedure. We have tested the corresponding wind speed every 25 V from 75 V to 200 V and recorded the data. We have tested the corresponding wind speed every 25 V from 75 V to 200 V and recorded the data for later reference. Similarly, we also turned the boomerang motor to different level and get the relationship between boomerang's angular velocity and its setting by recording its rotation and get its angular velocity in every degree from the video. Then change the voltage and repeat such procedure.

Since the reading of the electronic scale fluctuates consistently, when recording the readings, we used camera's burst mode to capture about 20 pictures and calculate their average as our scale reading.

Next, we placed the boomerang into the wind tunnel at its end and made it so the top side's rotating axis is along the wind, as shown in Figure 15.



Figure 15: Set up for trial 1 and 2

For the first trial, we set the boomerang's rotating speed at a certain point and change the fan from 75 V to 200 V at 25 V interval and record the corresponding reading of the electronic scale. For the second trial, we set the voltage of the fan at 150 V, and change the boomerang angular velocity and recorded the reading of the electronic scale. The rotation of the boomerang is recorded in video every time and the boomerang's angular velocity is derived from the video recording.

Then, we turned the rectangular frame so it's perpendicular to the wind as shown in Figure 16.



Figure 16: Set up for trial 3, 4, 5

Under this condition, the change in scale's reading is resulted mainly from the drag force the setup experiences. We used this set up conducted trial three, four and five. In trial three, we tested the corresponding weight change of different wind speed when the boomerang has no angular velocity. In trial four, we kept the angular speed unchanged and varied the wind speed; and in trial five, we set the fan input to 100 V and changed the boomerang's angular speed.

3.2 Data Analysis

3.2.1 Trail 1, 2 and lift coefficient

In the experiment, we have gathered data of relations between the change of the electronic scale's reading Δm and the wind velocity(v_h) or the boomerang's angular velocity(ω). The weight change is a result of a upward force exerted by the string which is cause by the frame's top board's rotation. When this setup reaches its equilibrium, the torque exert on the top board by the weights should equal to the torque generated by the uneven lift force on boomerang's two arms. Thus, we can use the tension on the string and its arm of force to calculate the torque:

$$\tau_L = \Delta m g l_w \quad (20)$$

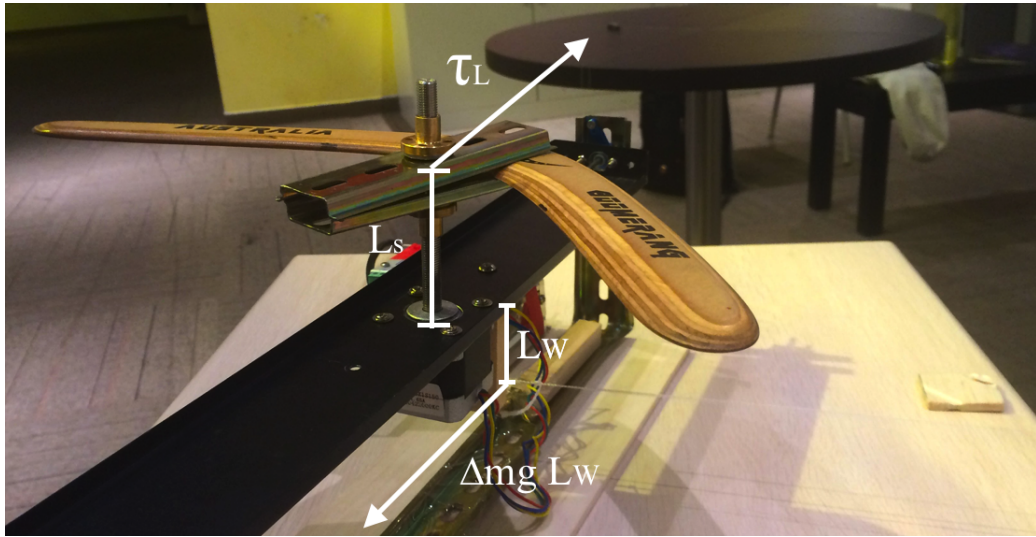


Figure 17: Torque diagram for trail 1 and 2

According to the data we gathered from trail 1 and 2, as in Figure 18 and 19,

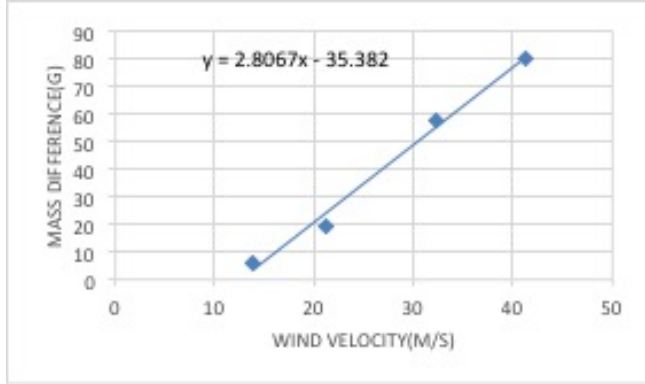


Figure 18: Δm vs. v_h

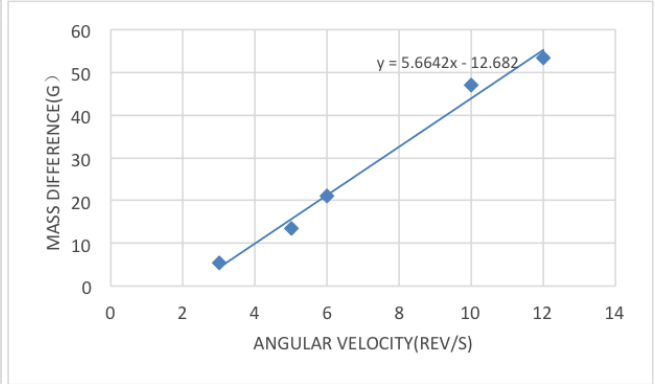


Figure 19: Δm vs. ω

when ω stays constant, Δm and v_h show a linear relation. Similarly, when v_h stays constant, Δm and ω show a linear relation as well. Figure 12 and 13 shows these relations in graphs.

According to the theoretical model $\tau_L = \rho C_L A (\frac{1}{3} v_h r^2 \omega)$ in previous sections and that $\tau_L = \Delta m g l_w$:

$$\Delta m g l_w = \frac{1}{3} \rho C_L A v_h r^2 \omega \quad (21)$$

In this case, the air density ρ , the area of boomerang's arm A , block's length l_w and the arms' length r all remain constant. Therefore, when v_h is unchanged, ω and Δm should have a linear relationship, and it's the same when τ_L is controlled and v_h varies, which corresponds to the relationships we got from the experiment. Thus, the experimental result supports our theory.

In trail 1, when the boomerang's angular velocity is set to 13 rev/s, the slope k_1 of the line Δm vs. v_{wind} is 0.5613. Assume the air density is standard $\rho = 1.293 \text{ kg/m}^3$, and, according to measurements, $A = 143.1 \times 10^{-4} \text{ m}^3$,

$l_w = 7.4\text{cm}$ and $r = 0.234\text{m}$. Thus, we can calculate the value of C_L :

$$\begin{aligned}
 C_L &= \frac{3\Delta m g l_w}{\rho A v_h r^2 \omega} \\
 &= \frac{3k_1 g l_w}{\rho A r^2 \omega} \\
 &= \frac{3(2.8067 \times 10^{-3})(10)(0.074)}{(1.293)(143.1 \times 10^{-4})(0.21 * 0.21)(26\pi)} \\
 &= 9.35 \times 10^{-2}
 \end{aligned} \tag{22}$$

Similarly, in trail 2, $k_2 = 1.1328$, $v_h = 32.3\text{m/s}$, so:

$$\begin{aligned}
 C_L &= \frac{3\Delta m g l_w}{\rho A v_h r^2 \omega} \\
 &= \frac{3k_2 g l_w}{\rho A r^2 v_h} \\
 &= \frac{3(5.664 \times \frac{10^{-3}}{2\pi})(10)(0.074)}{(1.293)(143.1 \times 10^{-4})(0.21 * 0.21)(32.3)} \\
 &= 7.59 \times 10^{-2}
 \end{aligned} \tag{23}$$

The average C_L is calculated to be 8.47×10^{-2} .

3.2.2 Trail 4, 5 and drag coefficient

In trail 4 and 5, the top board of the frame was put perpendicular to the wind. Therefore, the tension on the string was a result of the drag force of the wind. In trail 4, however, the result is not helpful: it is supposed to be a quadratic function which the quadratic coefficient should be positive but in our experiment, it is negative. We abandon trail 4 and conjecture that the strong wind actually moves the whole testing apparatus thus make it impossible to obtain useful results.

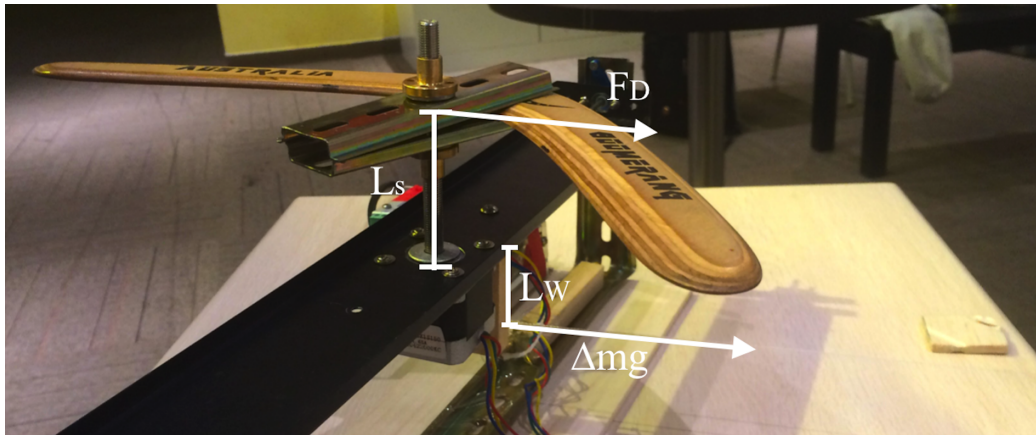


Figure 20: Force diagram for trail 4 and 5

As for trail 5, we've measured how Δm changes according to different v_h . According to our theoretical model,

$$F_D = \rho C_D A (v_h^2 + \frac{1}{6} r^2 \omega^2) \tag{24}$$

Thus, as in Figure 21,

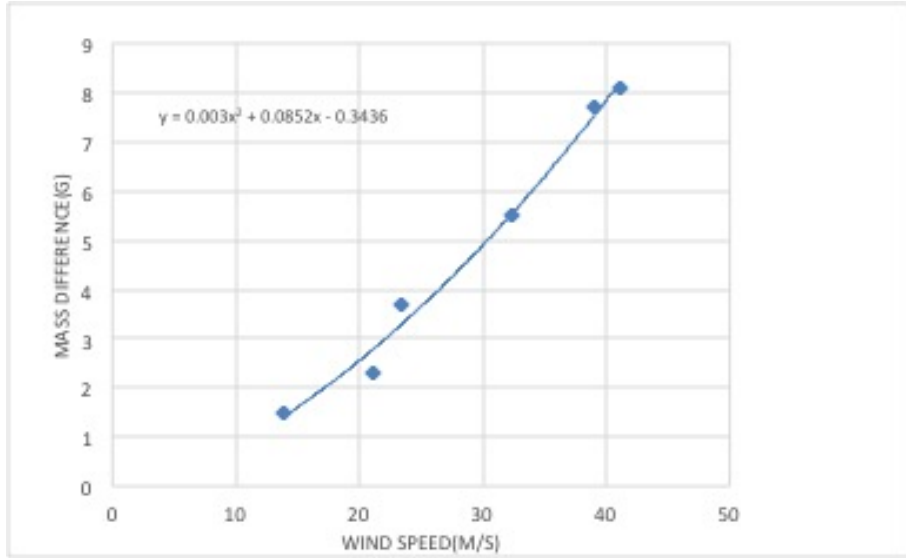


Figure 21: Δm vs. v_h

when ω is constant, Δm and v_h show a quadratic relation. Also, as we mentioned earlier:

$$\tau_L = \Delta m g l_w \quad (25)$$

Thus:

$$l_s \cdot [\rho C_D A (v_h^2 + \frac{1}{6} r^2 \omega^2)] = \Delta m g l_w \quad (26)$$

where l_s is the distance from boomerang's center of mass to the top board's rotating axis and $l_s = 0.051m$.

In trial 5, ω is constant, and the quadratic coefficient k_3 between Δm and v_h is $0.003g \cdot s/m$, therefore, we can calculate C_D from the equation above.

$$k_3 = \frac{l_s \rho C_D A}{g l_w} \quad (27)$$

$$\begin{aligned} C_D &= \frac{k_3 g l_w}{l_s \rho A} \\ &= \frac{(0.003 \times 10^{-3})(10)(0.074)}{(0.051)(1.293)(143.1 \times 10^{-4})} \\ &= 0.2352 \times 10^{-2} \end{aligned} \quad (28)$$

3.2.3 Error analysis

The numerical results of this experiment is legible but not very precise. For the two C_L measured in trail 1 and 2 using different methods, the error rate is:

$$\Delta_{error} \approx \frac{C_{L_1} - C_{L_2}}{\frac{1}{2}(C_{L_1} + C_{L_2})} \times 100\% = 20.72\% \quad (29)$$

The main cause of error would be the inconsistency of the wind. On the one hand, the intensity of wind doesn't necessarily correspond to the fan's input voltage in a measurable manner; also, the tunnel design can't completely reduce the influence of vortex and irregular flow. Besides, the experiment doesn't take into account the drag force exerted on measuring equipments by the wind.

3.2.4 Solve differential equation using Mathematica

Knowing the value of C_D and C_L , Wolfram Mathematica is able calculate the numerical solution of simplified differential equation of $\omega(t)$ and $v_h(t)$.(equation 13 and 14 in section 2.6)

$$-\frac{d\omega}{dt} \approx \frac{\rho C_D A}{I} \left(\frac{1}{4} v_h^2 r + \frac{1}{4} r^3 \omega^2 \right) \quad (30)$$

$$-\frac{dv_h}{dt} \approx \frac{\rho C_D A}{m} \left(v_h^2 + \frac{1}{6} r^2 \omega^2 \right) \quad (31)$$

$v/(m/s)$ or $\omega/(1/s)$

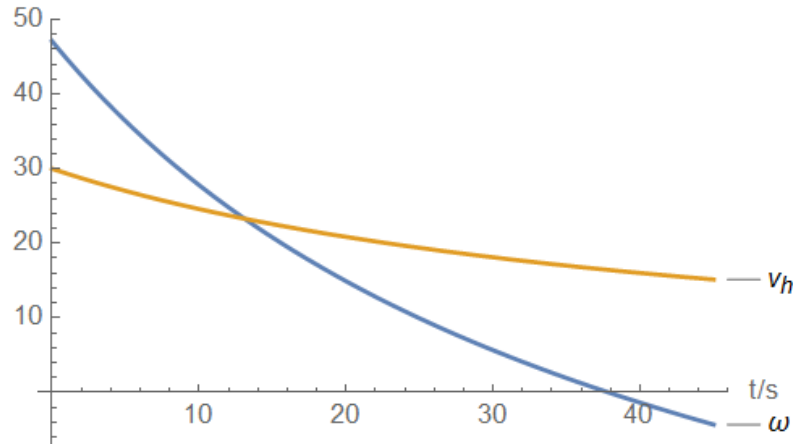


Figure 22: v_h/ms^{-1} and $\omega/rads^{-1}$ vs. time/s

The yellow line is the function of $\omega(t)$ and the blue line is the function of v_h . In this graph, both of the ω and v_h decrease as time increase, and $\omega=0$ when $t = 5.4s$, so the maximum flying time of the boomerang is not more than 5.4s.

Since we know the function of $\omega(t)$ and v_h . If it is supposed that α is a constant number, then Mathematica can solve the equation for the magnitude of \vec{R} as a function of t (equation 11 in section 2.6)

$$F_L \cos \alpha = m \frac{v_h^2}{|\vec{R}|} = \rho C_L A \left(\frac{1}{2} v_h^2 + \frac{1}{3} r^2 \omega^2 \right) \cos \alpha \quad (32)$$

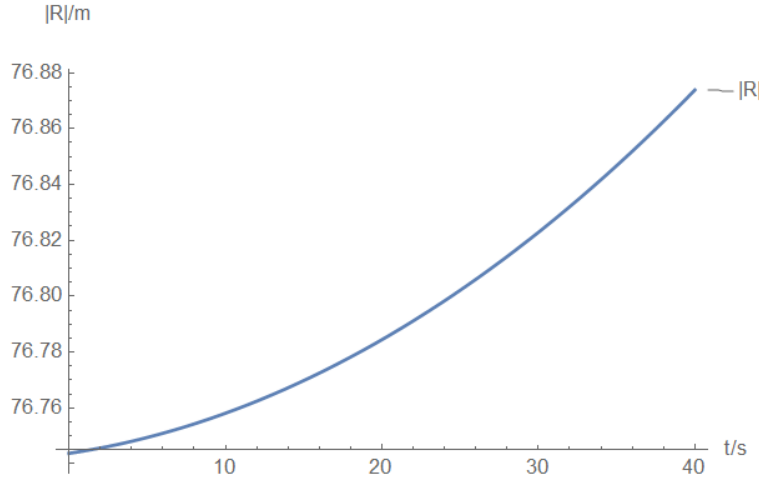


Figure 23: $|\vec{R}|/\text{m}$ vs. time/s

The $|\vec{R}|$ is almost invariant in this graph, but it is increasing rapidly in our observation. This indicate that α should not be seen as a constant. If α is increasing, as we observed, the graph of $|\vec{R}|(t)$ will be more accurate. To solve this problem, the experiment account for the changing α is designed in next section.

We also have another approach to calculate $|R|$, as demonstrated in chapter 2.6:

$$\beta(t) = \int_0^t \frac{\rho C_L A v_h r^2 dt}{3I \cos \alpha} \quad (33)$$

and the numerical solution is:

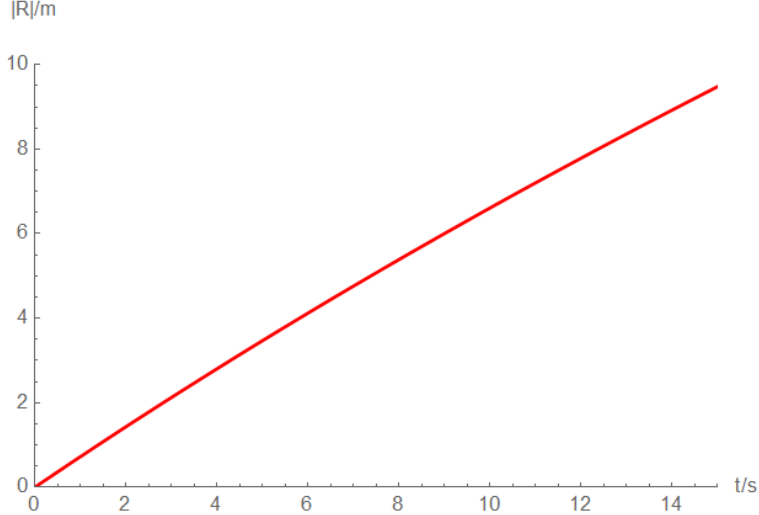


Figure 24: Numerical solution of $\beta(t)$

When $\beta = 2\pi$, the boomerang complete one circle of the trajectory, the t to make β become 2π is the hang time, in the numerical solution, it is 10. $|R|$ is approximately $\frac{V_h t}{2\pi} \approx 17$, which differs a lot from the force approach. This weird phenomenon is explained in next section.

3.2.5 Approaches to account for the Different result of $|R|$

2 approaches of changing α is critical to help you have a better understanding of why $|R|$ is not invariant. In section 2.3, the first approach is introduced, which is, the different C_L of two arms provides a torque that increase α . Another approach sees the flying boomerang as a gyroscope, and a gyroscope have the following property

$$|\vec{R}| = \frac{v_h(t)}{\frac{\tau_L(t)}{I\omega(t)}} = \frac{v_h(t)I\omega(t)}{\tau_L(t)} \quad (34)$$

This equation is equivalent to the β function above. It can be utilized to calculate $|\vec{R}|$. However, there is another approach associate with centripetal force that had been derived: $F_L \cos \alpha = m \frac{v_h^2}{|\vec{R}|}$. This two equations contradict each other, because one is dependent on $\alpha(t)$ while the other is independent, using different methods the plot of trajectory is also different. It is because they are in difference reference frame: the centripetal force equation refers to the observer while the gyroscope equation refers to itself. Therefore, the gyroscope equation explains how the angle of \vec{R} change refers to itself, i.e. the rate of change of the angle between $\vec{\omega}$ and x axis.

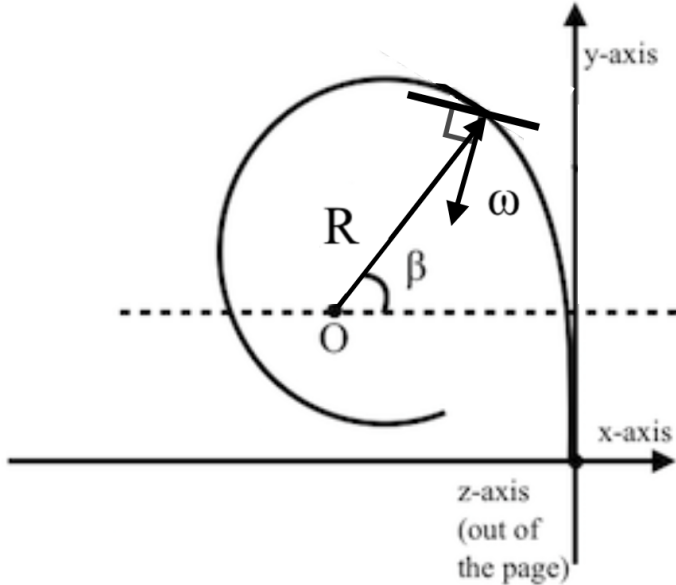


Figure 25: Difference between β and β'

The figure above gives a visual interpretation. As the $|R|$ is not invariant in both frames, the boomerang's plane must created an angle between the tangent line. This angle is the angle of attack, The air tends to apply a torque and a force: The torque decrease α but the effect of different C_L on two arms have a larger torque that counterbalance the torque provide by the air and increase α thus overall α increases. The force provided by the air complements the centripetal lift force provided by the boomerang itself thus place the actual radius function between two contradictory numerical solution of $|R|$ on the previous section.

3.3 Experiment account for $\alpha(t)$

3.3.1 Experiment objective

The data analysis above is base on that α is a constant. But, the change of α is a critical factor to simulate the trajectory of boomerang. The analytical formula of α cannot be derived in theoretical model ergo the experiment is constructed to figure out the numerical solution of $\alpha(t)$. Knowing $\alpha(t)$, one will not only have a better simulation, but also have the ability to verify whether the theoretical basis is correct.

3.3.2 Experiment setup

From a point O, the coordinate system is established. The whole flying process is recorded by two cameras in slow motion. One of the camera is fixed on 20 meters above point O, and the other camera is fixed on 20 meters left from O. The thrower's position is (10, -5) so that the whole trajectory is in both camera's vision. The setup is shown in the following diagram:

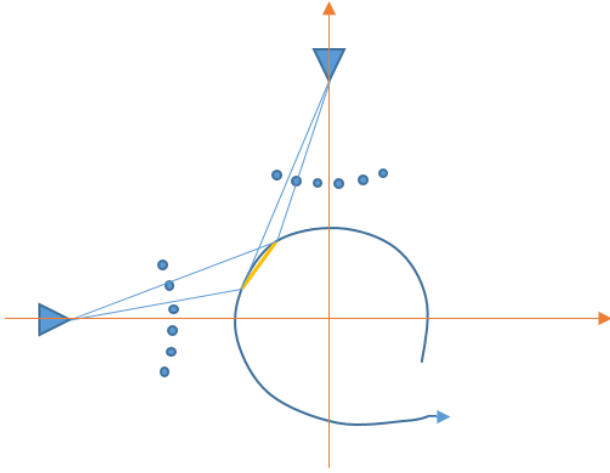


Figure 26: Experiment Setup

The blue triangles are cameras, the dots are poles, the blue circle-like line is the trajectory of boomerang, and the yellow line is the approximation path the boomerang travel during a certain interval. Using the poles as protractor, the angle between the two ends of the path and the angle between the axis and one end of the path is measured.

3.4 Data Calculation

The total hang time of the boomerang is recorded as t_1 . t_1 is divided into 10 time intervals, the number of rounds the boomerang rotates in each interval is recorded and ω is calculated. The horizontal distance the boomerang travels is estimated with a little trick: there are poles on the ground in front of each camera which can help them determine how much angle the boomerang traveled in a certain time interval.

With 2 cameras at fixed position, we can calculate the distance traveled in each time interval thus calculate v_h . The following figure is the mathematical model of the experiment.

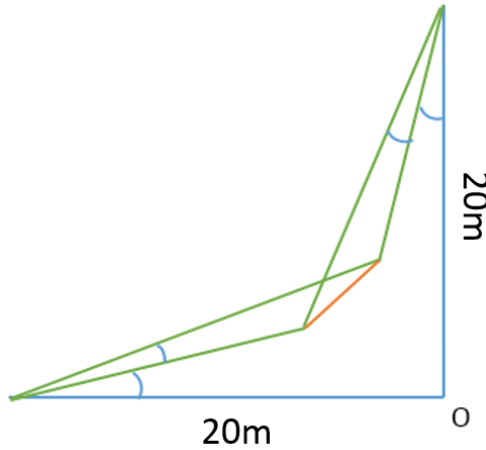


Figure 27: Mathematical Model

The angle marked in it has been measured thus the analysis formula of the green lines in the figure can be derived. After that, the coordinate of the two ends of the path and the distance between them is calculated.

From the experiment above we can get 10 coordinates of (t, ω) and 10 coordinates of (t, v_h) . Fit the line with 5th order polynomial. We could get a proper approximation of $v_h(t)$ and $\omega(t)$. In the data analysis section, these functions will be compared to the $v_h(t)$ and $\omega(t)$ that derived from theoretical model.

Since we know the coordinates of any ends of any path, we can also calculate $|R|(t)$ from the information that we have known, but the method is somewhat complex.

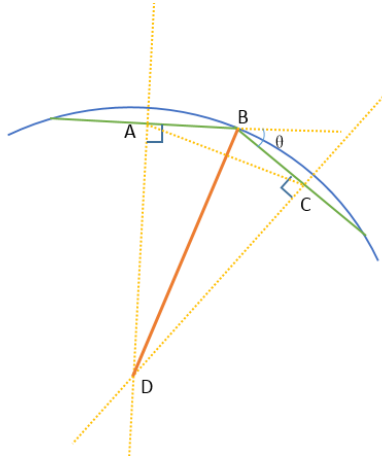


Figure 28: Mathematical Model to Calculate $|R|$

As shown in the diagram above, the green lines are approximation paths for 2 time intervals. AD and CD are perpendicular bisector of these paths. Thus, D is the center of this arc section and DB is the instantaneous radius of curvature between these 2 time intervals; therefore, we get 9 radius value. Each path have different angle to x-axis, the change of angle between two path is known, and the length AB, BC is known because they

are half of the path length. Apply the law of sines and the law of cosines:

$$\frac{AC}{\sin(\theta)} = R$$

$$AC^2 = AB^2 + BC^2 - 2AB \times BC \times \cos(\pi - \theta)$$
(35)

Combine those equations,

$$R^2 \sin^2(\theta) = AB^2 + BC^2 + 2AB \times BC \times \cos(\theta)$$

$$R = \sqrt{\frac{AB^2 + BC^2 + 2AB \times BC \times \cos(\theta)}{\sin^2(\theta)}}$$
(36)

This equation can be used to determine the value of $|R|$.

3.5 Data analysis

We calculate the coordinates of all 11 points from the original data:

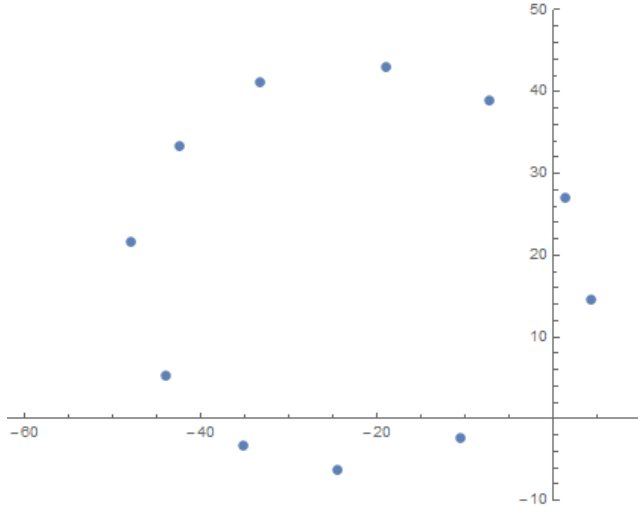


Figure 29: Dot plot of the trajectory

The trajectory seems to be a ellipse, and our objective to analyze this data is to find a general simulation. The simulation must be approximately close to this particular case which $\omega_0 = 47.1$, $v_{h0} = 30.0$, and have the ability to predict the trajectory when the initial value is different. But before we get a generalized theory, the proof of each part of the theory in the theoretical model is necessary.

3.5.1 Verification of the theoretical model of $\omega(t)$ and $v_h(t)$

In the experiment, we get a set of 10 values of $\omega(t)$ and $v_h(t)$, the data is fitted using 2-order polynomial, and the fit graph is compared to the theoretical model.

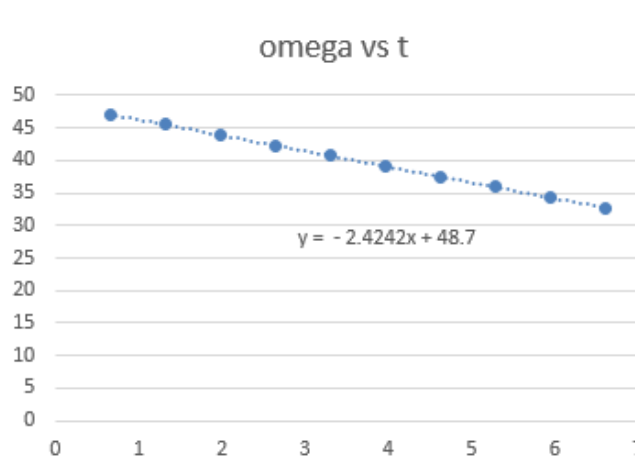


Figure 30: ω data fit

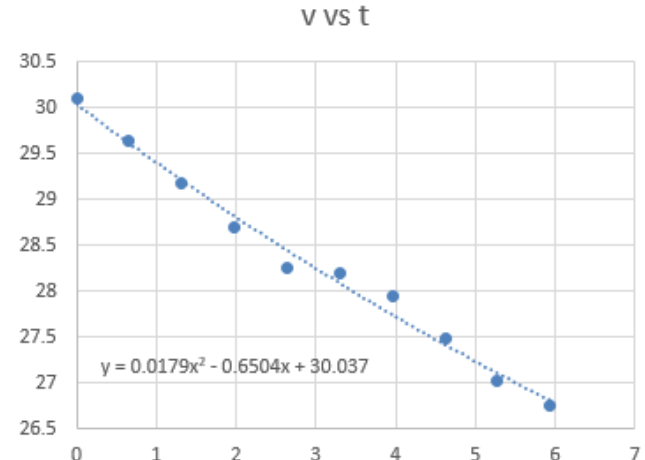


Figure 31: v_h data fit

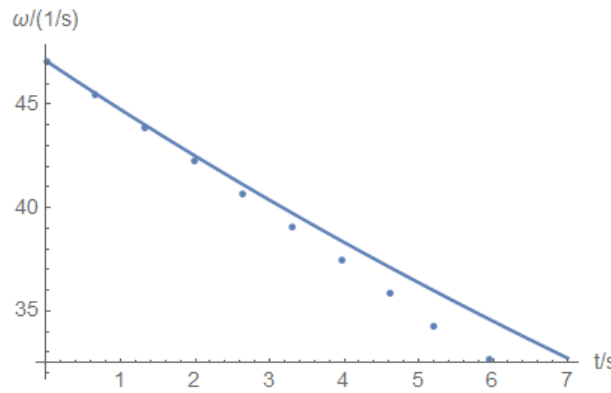


Figure 32: ω comparison

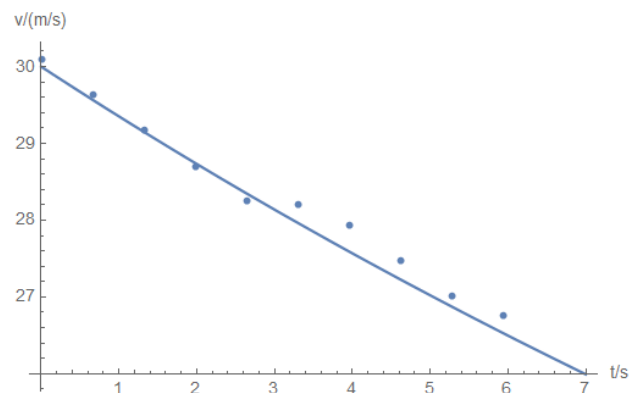


Figure 33: v_h comparison

The blue dots in both of these comparisons are data approximation, and the blue lines represents theoretical model.

In the total hang time range, ω in the theoretical model never differ from the data more than 5%. Surely theoretical model provide a successful approximation of ω , and the horizontal velocity is even more precise. Ergo the model of ω and v_h is verified.

3.5.2 Numerical solution of $|R|$ and α

$|R|$ at each of the 9 points is calculated and displayed in the following graph, and the analytical formula of the 4th order fit is also calculated and displayed.

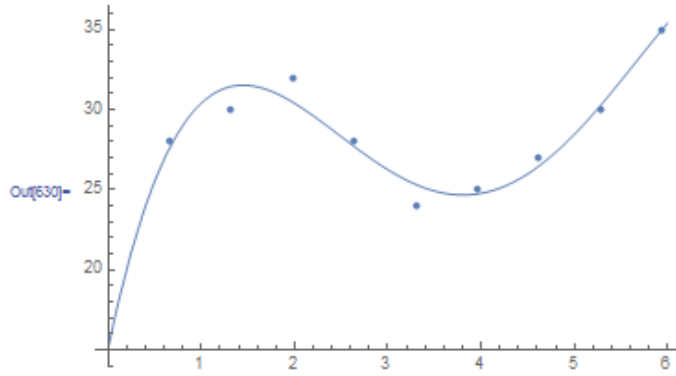


Figure 34: 4th order solution of $|R|$

$$|R| = 15.1111 - 27.7547t + 15.2279t^2 - 2.94814t^3 + 0.1812t^4 \quad (37)$$

The following is an approximation of $\cos \alpha$. It is clear in the diagram that alpha is approximately $\frac{\pi}{2}$ at $t = 6.6s$. This is what we expected because we observe that the boomerang becomes nearly horizontal at the end of its flight.

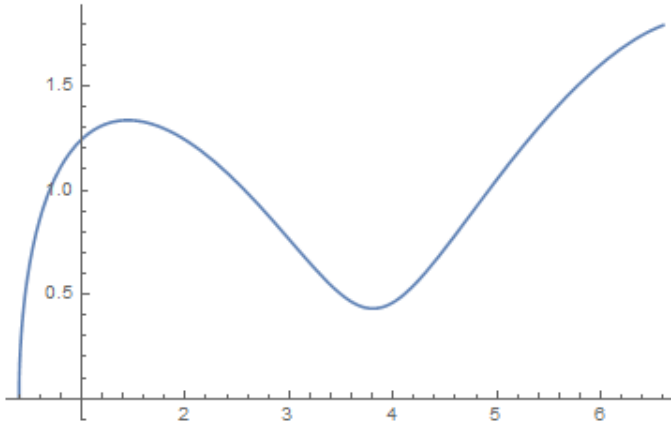


Figure 35: Solution of alpha

As we have known the numerical solution of ω , v_h and $|R|$. The numerical solution of α is also evaluated using the formula:

$$F_L \cos \alpha = m \frac{v_h^2}{|\vec{R}|} = \rho C_L A \left(\frac{1}{2} v_h^2 + \frac{1}{3} r^2 \omega^2 \right) \cos \alpha \quad (38)$$

As we gain the numerical solution of α . The motion on z-axis is also solved using the equation:

$$\begin{aligned}
 z(t) &= \int_0^t v_v(t) dt \\
 z(t) &= \int_0^t \int_0^t \frac{F_v}{m} dt dt \\
 z(t) &= \int_0^t \int_0^t \left(\frac{F_L \sin \alpha}{m} - g \right) dt dt \\
 z(t) &= \int_0^t \int_0^t \left(\frac{\rho C_L A}{m} \left(\frac{1}{2} v_h^2 + \frac{1}{3} r^2 \omega^2 \right) \cos \alpha \sin \alpha - g \right) dt dt
 \end{aligned} \tag{39}$$

3.5.3 Simulation

As the radius of curvature and the horizontal speed is known, the overall trajectory is simulated and visualized base on the following equation.

$$\frac{1}{R} = \frac{|x'(t)y''(t) - x''(t)y'(t)|}{(x'^2(t) + y'^2(t))^{3/2}} \tag{40}$$

which x and y are the coordinates on xy plane, this equation combined with the equation $x'(t)^2 + y'(t)^2 = v_h^2$, the differential equation could be solved numerically. With that solution, the trajectory, which is the parametric equation of x ,y as a function of t can be plotted.

Knowing the basic principle, a program based on Mathematica is designed to construct the parametric equation with certain inputs of the initial value of ω and, v_h . The codes are in the appendix.

The trajectory simulation of the boomerang when $\omega_0 = 47.1, v_{h0} = 30.0$ is like this (the left figure):

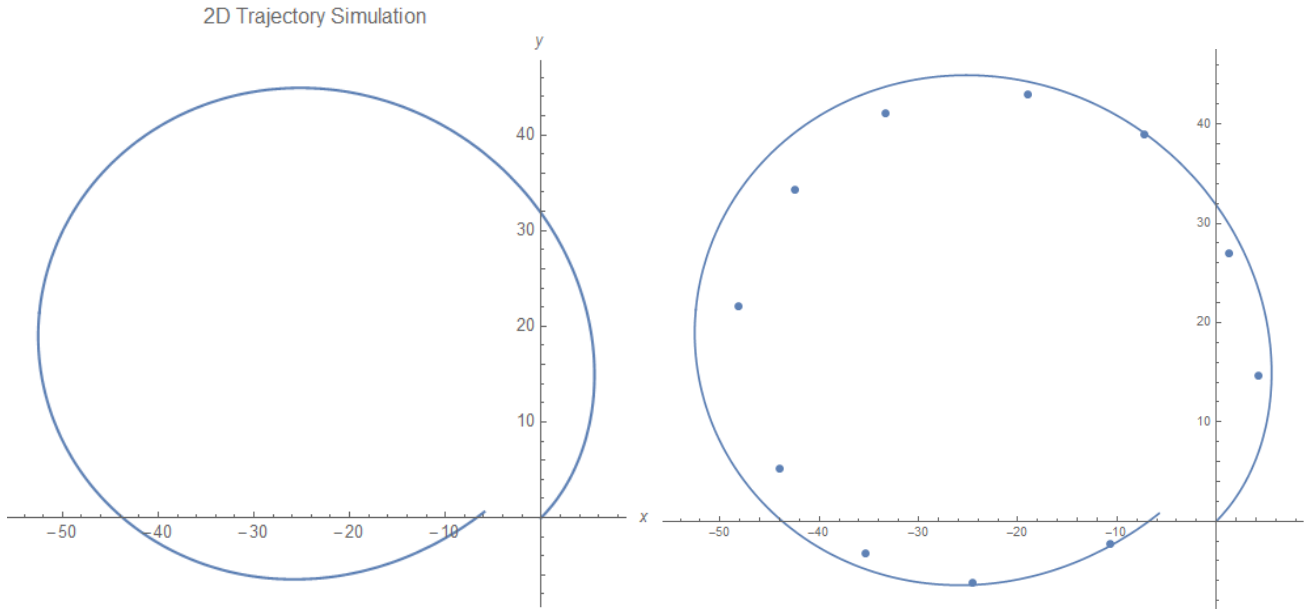


Figure 36: 2D Trajectory simulation

Figure 37: Comparison with original data

It is not only intuitively correct, when it is compared to the original data, it is concluded that this approximation is precise enough because the maximum error is only about 5%.

But one-shot could not prove that the program is trustworthy, so another field experiment is constructed. If the data calculated in this experiment matches the prediction of the program, then this program is proved to be credible.

The initial value are $\omega = 42.1$, $v_{h0} = 23.7$ and the comparison of data and program prediction is like this:

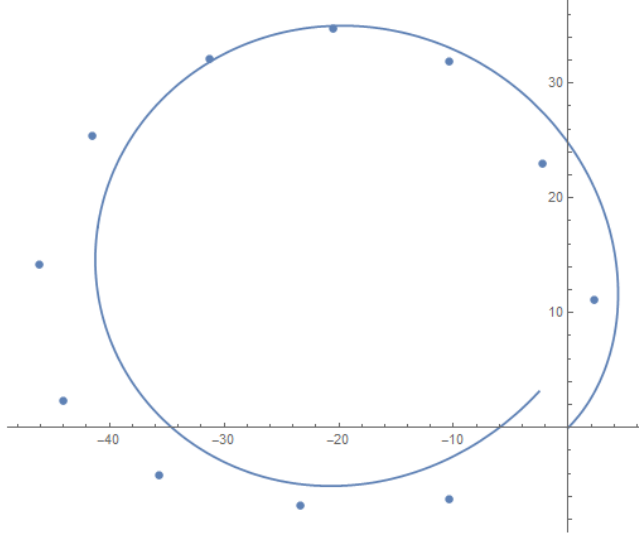


Figure 38: second comparison

It may seems a little deviant to the left, but since the position of the thrower is arbitrary, the dot plot could be shifted leftward to match the prediction. This result indicate that the the program is reliable.

3.5.4 Significance

The best simulation of all the previous studies is Hunt's trajectory simulation, which differs with ours a lot. It is because we consider several parameters as a function of time. The comparison between his result and ours is shown in the graph below:

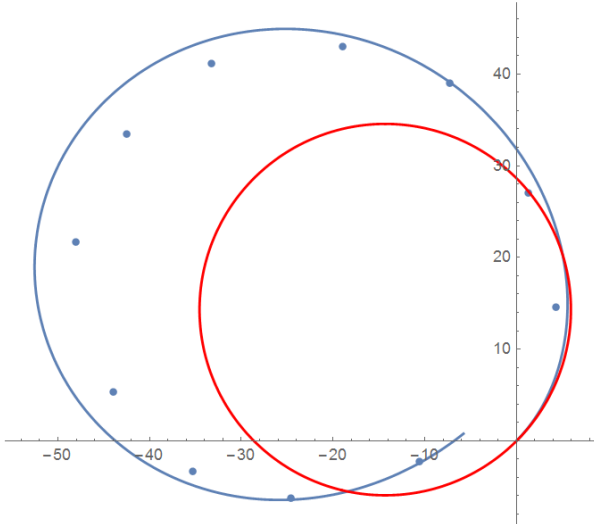


Figure 39: Comparison when $\omega_0 = 47.1, v_h = 30.0$

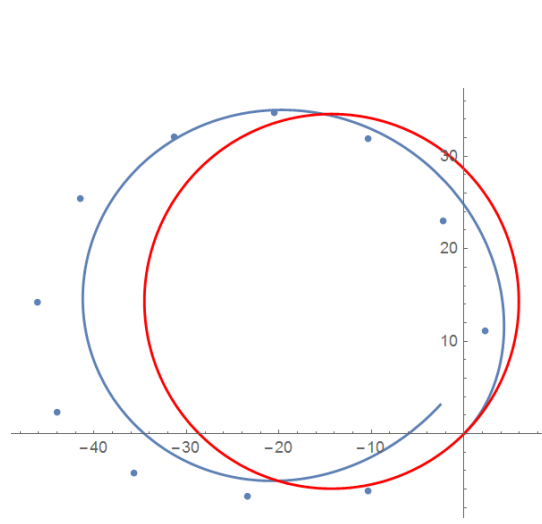


Figure 40: Comparison when $\omega_0 = 47.1, v_h = 30.0$

The red line is Hunt's simulation, which is a simple circle with a radius as a function of lift coefficient. Clearly, our simulation is more accurate.

4 Conclusion

In our theoretical model of the trajectory of a boomerang, we address some variables that have been previously studied, and some that have not. We use time functions of vertical displacement, horizontal velocity, and vector radius to model one particular three dimensional trajectory for every boomerang with the same properties and thrown with same initial conditions.

We then simplify our theory to make feasible the experiment that measures lift and drag coefficients of our specific boomerang. The results for these are within reasonable range.

In our second experiment, we take in to account change in angle of inclination, and change in radius which are not accounted for in the first experiment. Through this, we are able to verify our theoretical model. This experiment also helps us to build a Mathematica program to simulate the trajectory of a boomerang by imputing initial horizontal and angular velocities. The simulation result is way more accurate than the previous study.

5 Appendix

5.1 Mathematica Codes

the initial value of ω is 47.1 rad/s
 the initial value of v_h is 30 m/s

$\omega(t)$ and $v_h(t)$:

```
s = NDSolve[{y'[t] == -(1.293*0.002352*0.01431)/(9451.6*10^(-7))*((z[t])^2*0.21/4 + 0.21^3/4*(y[t])^2), z'[t] == -(1.293*0.002352*0.01431)/0.06019*((z[t])^2 + 0.21*0.21/6*(y[t])^2), y[0] == 47.1, z[0] == 30}, {y[t], z[t]}, {t, 45}]
Plot[Evaluate[{y[t], z[t]} /. s], {t, 0, 45}, PlotRange -> All]
```

$|R|(t)$ when α is constant:

```
s = NDSolve[{y'[t] == -(1.293*0.002352*0.01431)/(9451.6*10^(-7))*((z[t])^2*0.21/4 + 0.21^3/4*(y[t])^2), z'[t] == -(1.293*0.002352*0.01431)/0.06019*((z[t])^2 + 0.21*0.21/6*(y[t])^2), y[0] == 47.1, z[0] == 30}, {y[t], z[t]}, {t, 45}]
Plot[Evaluate[{y[t], z[t]} /. s], {t, 0, 45}, PlotRange -> All]
```

$\beta(t)$:

```
s = NDSolve[{y'[t] == -(1.293*0.002352*0.01431)/(9451.6*10^(-7))*((z[t])^2*0.21/4 + 0.21^3/4*(y[t])^2), z'[t] == -(1.293*0.002352*0.01431)/0.06019*((z[t])^2 + 0.21*0.21/6*(y[t])^2), y[0] == 47.1, z[0] == 30}, {y[t], z[t]}, {t, 40}];
f[x_] := Integrate[1.293*0.084705*0.01431*(z[t] /. s)*0.21*0.21/(3*9451.6*10^(-7)), {t, 0, x}];
Plot[f[x], {x, 0, 20}, PlotStyle -> {Red, AbsoluteThickness[2]}, PlotLabel -> y?f[x], PlotRange -> {{0, 15}, {0, 10}}]
```

ω comparison:

```

s = NDSolve[{y'[t] == -(1.293*0.002352*0.01431)/(9451.6*10^(-7))*((z[t])^2*0.21/4 + 0.21^3/4*(y[t])^2),
z'[t] == -(1.293*0.002352*0.01431)/0.06019*((z[t])^2 + 0.21*0.21/6*(y[t])^2),
x[t] == -2.424 t + 47.1, y[0] == 47.1, z[0] == 30}, {y[t], z[t], x[t]}, {t, 45}]
Plot[Evaluate[{y[t], x[t]} /. s], {t, 0, 6.6}, PlotRange -> All]

```

v_h comparison:

```

s = NDSolve[{y'[t] == -(1.293*0.002352*0.01431)/(9451.6*10^(-7))*((z[t])^2*0.21/4 + 0.21^3/4*(y[t])^2),
z'[t] == -(1.293*0.002352*0.01431)/0.06019*((z[t])^2 + 0.21*0.21/6*(y[t])^2),
x[t] == 0.0179 t^2 - 0.6504 t + 30.037, y[0] == 47.1, z[0] == 30.1}, {y[t], z[t], x[t]}, {t, 45}]
Plot[Evaluate[{z[t], x[t]} /. s], {t, 0, 6.6}, PlotRange -> All]

```

|R| data:

```

f = ArcCos[(z[t] /. s)^2*0.06019/(rr*1.293*0.084705*0.01431 (0.5 (z[t] /. s)^2 + 1/3*0.21*0.21*(y[t] /. s))) - 2.2]
Plot[Evaluate[f], {t, 0, 6.6}, PlotRange -> All]
fa := {{0.66, 28}, {1.32, 30}, {1.98, 32}, {2.64, 28}, {3.3, 24}, {3.96, 25}, {4.62, 27}, {5.28, 30}, {5.94, 35}}
ga := ListPlot[fa, PlotRange -> {{0, 10}, {0, 40}}]
rr = Fit[fa, {1, t, t^2, t^3, t^4}, t]
Plot[rr, {t, 0, 6}]
Show[rr, ga]

```

Trajectory simulation:

```

a = Input[];
b = Input[];
s = NDSolve[{omega'[t] == -(1.293*0.002352*0.01431)/(9451.6*10^(-7))*((vh[t])^2*0.21/4 + 0.21^3/4*(omega[t])^2),
vh'[t] == -(1.293*0.002352*0.01431)/0.06019*((vh[t])^2 + 0.21*0.21/6*(omega[t])^2), omega[0] == a,
vh[0] == b}, {omega, vh}, {t, 45}];
fa := {{0.66, 28}, {1.32, 30}, {1.98, 32}, {2.64, 28}, {3.3, 24}, {3.96, 25}, {4.62, 27}, {5.28, 30}, {5.94, 35}};
rou = Fit[fa, {1, t, t^2, t^3, t^4}, t];
rouu = rou*b^2/a^2*2218.41/900;
lp =
ListPlot[{{4.3, 14.6}, {1.3, 27}, {-7.3, 39}, {-19.0,

```

```

43}, {-24.6, -6.2}, {-33.3, 41.1}, {-42.5, 33.43}, {-48.1,
21.64}, {-44, 5.3}, {-35.3, -3.3}, {-10.63, -2.3}],  

PlotRange -> {{-50, 10}, {-10, 50}}];  

alpha = ArcCos[(vh[t] /.  

s)^2*0.06019/(rou*1.293*0.084705*0.01431 (0.5 (vh[t] /.  

s)^2 + 1/3*0.21*0.21*(omega[t] /. s))) - 2.2];  

vh = (Round[1000 (vh[2] - vh[0])]/1000*t/2 + Round[10 vh[0]]/10) /.  

s[[1]];  

omeg = (Round[1000 (omega[2] - omega[0])]/1000*t/2 +  

Round[10 omega[0]]/10) /. s[[1]];  

sol =  

NDSolve [  

{xxaa'[t]^2 == vhh^2 - yyaa'[t]^2 ,  

rouu == vhh^3/Abs[xxaa'[t]*yyaa''[t] - yyaa'[t]*xxaa''[t]],  

xxaa[0] == 0, yyaa[0] == 0, xxaat[0] == b/1.414,  

yyaa'[0] == b/1.414}, {xxaa, yyaa}, {t, 6}];  

If[xxaa[3] < yyaa[3] /. sol[[1]],  

Plot[Evaluate[{xxaa[t], yyaa[t]} /. sol], {t, 0, 6}, PlotRange -> All]  

Show[ParametricPlot[Evaluate[{xxaa[t], yyaa[t]} /. sol], {t, 0, 6}],  

lp, PlotRange -> All]  

, Plot[Evaluate[{yyaa[t], xxaat[t]} /. sol], {t, 0, 6},  

PlotRange -> All]  

Show[ParametricPlot[Evaluate[{yyaa[t], xxaat[t]} /. sol], {t, 0, 6}],  

lp, PlotRange -> All]]

```

Works Cited

- Barceló, G. (2014). Theory Of Dynamic Interactions: The Flight Of The Boomerang. *Journal Of Applied Mathematics And Physics*.
- Bloch, A. (1990). Stabilization of rigid body dynamics by the Energy-Casimir method *ResearchGate*.
- Clarich, A. (2013). Multi-objective Optimization Of A Boomerang Shape. *University Of Trieste*.
- Hawes, L. L. (1987). All About Boomerangs.
- Hess, F. (1968). The Aerodynamics Of Boomerangs. *Scientific American*.
- Humble, S. (2006). Maths Circus: Boomerangs. *Teaching Mathematics And Its Applications*.
- Hunt, H. (2001). Ideal Behavior Of A Perfect Boomerang. *Cambridge University*.
- Kuleshov, A. (2010). A Mathematical Model Of The Boomerang. *ProcediaEngineering*.
- Pakalnis, S. (2006). Aerodynamics Of Boomerang. *Research Support Technologies*.
- Vassberg, J. C. (2012). Boomerang Flight Dynamics. *Aerodynamics Lecture*.
- Yihui, Jin, Shuangping, Li, Shuangning, Li. (2012).Construction and Stabilization of Small-scale Wind Tunnel. *Theoretical Research*.

Acknowledgements

A very special thanks to our friends, Liu, Zisen and Wang Shuyu, for lending us their wind tunnel and fan. Another special thanks to our beloved adviser, Guan Chun, and other physics teachers.